JOURNAL OF GEOPHYSICAL RESEARCH, VOL. 106, NO. C7, PAGES 13,903–13,915, JULY 15, 2001

Initiation of the spring phytoplankton increase in the Antarctic Polar Front Zone at 170°W

Michael R. Landry,[1] Susan L. Brown,[1] Karen E. Selph,[1] M.R. Abbott,[2]
R.M. Letelier,[2] Stephanie Christensen,[1] Robert R. Bidigare,[1] and K. Casciotti[3]

Abstract. During austral summer 1997, satellite imagery revealed enhanced chlorophyll associated with the Antarctic Polar Front at 170°W. Phytoplankton growth conditions during the early stages of the spring increase were investigated on the Antarctic Environment and Southern Ocean Process Study Survey I cruise using flow cytometry (FCM) and microscopy to characterize community biomass, composition and biological stratification and dilution experiments to estimate growth and grazing rates. Physical and biological measures showed a general shoaling of mixed layer depth from ~200 to <100 m from late October to early November. Plankton assemblages on the southern side of the frontal jet (~0°C waters) differed from those on the northern side (~2°C) in enhanced relative importance of larger (>20 μm) cells, greater contributions of diatoms and ciliates, and a twofold higher ratio of protistan grazers to photoautotrophs. Phytoplankton community growth rates from incubations at 10 and 23% of surface incident light showed good agreement between high-performance liquid chromatography estimates of chlorophyll *a* (Chl *a*) (0.20 d^{-1}) and FCM cell-based (0.21 d^{-1}) results. Fucoxanthin-based estimates for diatoms were 0.24 d^{-1}. Mean estimates of microzooplankton grazing from the three phytoplankton measures were 0.16, 0.12, and 0.11 d^{-1}, respectively. Heterotrophs typically consumed 40-100% of their body carbon per day and thus presumably grew at rates similar to phytoplankton. The low net rates of Chl *a* increase in shipboard bottle incubations (0.04 d^{-1}) were consistent with the slow downstream accumulation of phytoplankton biomass (0.03 d^{-1}) as measured with instrumented Lagrangian drifters through the month of November. Both were slightly less than the net rate estimates from SeaSoar surveys (0.05 d^{-1}) because of the effects of pigment photoadaptation (bleaching) during this time of increasing light level and water column stratification.

1. Introduction

The Antarctic Circumpolar Current (ACC) contains the largest reservoir of near-surface excess nutrients for phytoplankton growth in the oceans. Unlike other high-nutrient systems in the subarctic and eastern equatorial Pacific, however, phytoplankton biomass, measured as chlorophyll *a* (chl *a*), does not remain monotonously low throughout the ACC. During the austral summer, the Antarctic Polar Front (PF) often stands out in satellite imagery as a band of enhanced chlorophyll around Antarctica. This zone is typically distinct from other areas of elevated pigment that are closer to the continent and more strongly influenced by the seasonal melting of sea ice [*Moore et al.*, 1999]. One of the goals of the U.S. Joint Global Ocean Flux Study (JGOFS) Antarctic Environment and Southern Ocean Process Study (AESOPS) was to understand the regulation of phytoplankton biomass and growth in the Pacific sector of the PF at 170°W. Here we report on the growth conditions during the early stages of the spring phytoplankton increase in 1997.

A sharp temperature gradient and an intensification of the W-SW to E-NE flowing current mark PF surface waters at 170°W. The main axis of the current jet follows the Pacific-Antarctic Ridge crest and typically lies within the latitudinal range of 60°-61°S, although instabilities result in meanders of a degree or more [*Abbott et al.*, 2000]. In 1997, ocean color imagery from the Sea-viewing Wide Field-of-view Sensor (SeaWiFS) revealed a gradual chlorophyll accumulation in this region beginning approximately in the second week of November and peaking in mid-December [*Moore et al.*, 1999]. The early development of this feature was captured in observational and experimental studies on the AESOPS Survey I cruise from October 20 to November 24 aboard the R/V *Roger Revelle*.

Experimental activities on Survey I were somewhat limited by the cruise's principal objectives, deploying 12 current meter moorings in the front axis and SeaSoar mapping of its physical and biological features. Between these activities, however, intensive sampling and experimental work were conducted at several stations to characterize the plankton community biomass, composition, and biological stratification of the water column and to estimate the rates of phytoplankton growth, microzooplankton grazing, and net phytoplankton increase. The link between these point stock

[1]Department of Oceanography, University of Hawaii at Manoa, Honolulu, Hawaii.
[2]College of Oceanic and Atmospheric Sciences, Oregon State University, Corvallis, Oregon.
[3]Geosciences Department, Princeton University, Princeton, New Jersey.

Paper number 1999JC000187.
0148-0227/01/1999JC000187$09.00

and rate measurements and their consequences was provided by instrumented drifters, which followed the temporal development of the "local" phytoplankton increase as water was advected downstream.

2. Materials and Methods

2.1. Water Column Sampling

Basic hydrographic information (temperature, salinity, density, light, and nutrients) was obtained from profiles collected with a conductivity-temperature-depth (CTD)-rosette at each station and posted at the U.S. JGOFS website (http://usjgofs.whoi.edu). Daily averaged estimates of incident photosynthetically active radiation (PAR) were problematic on the Survey I cruise because the PAR sensor on the ship's integrated meteorological package was nonfunctional. To compensate for this deficiency, the pattern in surface incident light was approximated by downwelling irradiance at 490 nm (E_d490) measured by instrumented drifters (see below), beginning on November 8. Prior to that we used shipboard measurements of daily-integrated short-wave radiation as an E_d490 proxy by first computing the average ratio between short-wave and E_d490 estimates for the days during which the two measurements overlapped, then applying this ratio to other daily estimates of short-wave radiation.

Although the spectral composition of incoming sunlight changes as a function of solar angle and the relative proportions of direct and diffuse radiation, the narrowband (10 nm) measurement at 490 nm is highly correlated with the full spectrum of photosynthetically available radiation [*Kirk*, 1994; *Baker and Frouin*, 1987]. To convert E_d490, measured as μW cm^{-2} nm^{-1}, to the full PAR spectrum (400-700 nm), we used the spectral solar irradiance model of *Gregg and Carder* [1990] to determine a mean multiplication factor of 270 for the full daylight cycle. The resulting PAR estimates (μW cm^{-2}) were expressed in terms of quanta using the relationship 1W = 2.77 x 10^{18} quanta s^{-1} from *Kirk* [1994, p. 5].

Samples from CTD profiles were taken for analyses of abundance, biomass, and cellular fluorescence properties of phytoplankton and heterotrophic (nonplastidic) protists at five intensively sampled hydrographic stations (Table 1). The bottles were sampled for five community analyses: small (SV) and large volume (LV) samples analyzed by FCM, SV and LV samples prepared as slides and analyzed by epifluorescence microscopy, and whole water samples preserved with acid Lugol's fixative and analyzed by inverted microscopy (details below). Samples for high-performance liquid chromatography (HPLC) pigment analyses of the phytoplankton community were taken as part of growth and grazing experiments (below).

2.2. FCM Analyses

SV FCM samples (1 mL) were preserved with 0.5% paraformaldehyde (final concentration), frozen in liquid nitrogen, and stored at -85°C (shipped in dry ice) until analysis in our shore-based laboratory. Frozen samples were thawed and stained in the dark with Hoechst 33342 (1 μg mL^{-1}) for 1 hour, and 100 μL subsamples were enumerated with a Coulter EPICS 753 flow cytometer equipped with dual 5W argon lasers, Microsample Delivery System II automatic sampling, a Biosense flow cell and CICERO Cytomation software [*Monger and Landry*, 1993]. Standard beads (0.57 and 0.98 μm YG Fluoresbrite microspheres for visible excitation and 0.46 μm UV excitable beads, Polysciences) were added to each sample as a basis for normalizing fluorescence signals. The dual lasers were aligned colinearly with the first tuned to the UV range at 225 mW to excite Hoechst-stained DNA. The second was tuned to 488 nm at 1.0 W to elicit red autofluorescence of chlorophyll-containing cells. Forward angle light scatter (FALS), right angle light scatter (RALS), and four fluorescence signals were collected for each cell, stored in list mode files, and analyzed using CYTOPC software [*Vaulot et al.*, 1989]. *Synechococcus* spp. cells were distinguished from other autotrophic cells in SV FCM analyses by their relatively small size (FALS) and orange autofluorescence.

Our original intention was to analyze LV FCM samples shipboard, immediately after collection and without preservation. Because of a laser failure on the Survey I cruise, however, most of the samples were preserved first (0.5% paraformaldehyde and frozen as above) and processed after the cytometer was repaired. For samples processed live (station 8), seawater (250 mL) was collected in dark polypropylene bottles and kept in an ice bath until analysis (within 1-2 hours). The shipboard flow cytometer was a Coulter EPICS Profile II with a 488 nm argon air-cooled laser (35 mW), a BioSense flow cell with a 150 mm beam-shaping lens, and a 150 x 14 μm beam spot. This basic instrument was modified with a multiple rate infusion pump (Sage

Table 1. Locations and Mixed Layer Environmental Conditions of Intensively Sampled Hydrographic Stations During AESOPS Survey 1.[a]

Station	Date	Location	MLD	T, °C	S, ‰	N	P	Si
1	Oct. 24	57.0°S, 170.0°W	194	4.15	34.04	23.1	1.60	8.3
8	Nov. 1	60.5°S, 169.0°W	182	0.07	33.90	28.8	1.98	26.6
12	Nov. 5	59.3°S, 170.0°W	116	2.20	33.99	26.6	1.83	15.2
18	Nov. 14	60.2°S, 170.7°W	59	1.79	33.98	27.3	1.89	17.4
23	Nov. 18	60.8°S, 168.2°W	101	0.02	33.91	28.0	1.96	26.3

[a]All sampling dates are 1997. MLD defined as the depth (m) at which σ_t = surface σ_t + 0.01 kg m^{-3}. N, P, and Si are dissolved concentrations (μM) of the nutrients, nitrate, phosphate, and silicate.

Instruments, model 361) to handle sample volumes up to 60 mL and delivery rates up to 3 mL min^{-1}. The photomultiplier tube (PMT) array was also modified to collect cell-specific information on red autofluorescence (680 nm bandpass filter), RALS side scatter (488 nm dichroic lens), and vertical and horizontal FALS (50/50 dichroic and polarizing filters). Data acquisition was triggered by red fluorescence (chlorophyll-containing cell), and the files were collected in listmode using CyCLOPS software (Cytomation, Fort Collins, Colorado). Sample fluorescence and light-scattering properties were normalized by including 6 μm fluorescent microspheres (Polysciences 18862YG) in each sample. However, because some LV FCM samples were analyzed live and some were preserved, we report cellular fluorescence estimates from SV analyses, which were done in a consistent manner.

2.3. Microscopical Analyses

Cells in the nanoplankton size range (2-20 μm) were enumerated from 50 mL samples preserved with 2 mL of 10% paraformaldehyde and stained with 25 μL of proflavin. The samples were concentrated on 1 μm, 25 mm black polycarbonate membrane filters and stained with 4',6-Diamidino-2-phenylindole dihydrochloride (50 μg mL^{-1}) for 0.5 min in the final stages of filtration. Cells in the microplankton range (20-200 μm) were counted from 250 ml samples preserved and cleared with sequential additions of alkaline Lugol's fixative (0.005% final concentration), 0.05% borate-buffered formaldehyde, and 0.3% sodium isothiosulfate [*Sherr and Sherr*, 1993]. These samples were stained with proflavin, filtered onto 10 μm black polycarbonate membrane filters, and stained with DAPI as above. Filters from both preparations were mounted on glass slides with a drop of immersion oil and viewed shipboard with a video image analysis system before freezing at -70°C. The video system consisted of a Zeiss standard epifluorescence microscope on an antivibration platform, with a 100 W power supply, and C-mounted Zeiss 3 CCD video camera and ZVS-3C75DE processor. At least 20 random images per slide were digitized shipboard and downloaded to a PC computer with Zeiss Image Plus software. These initial images were the primary basis for subsequent analysis of autotrophic (chlorophyll containing) and heterotrophic (nonpigmented) abundances and biomass, with the original frozen slides serving as backup.

Acid Lugols-preserved samples (250 mL) were taken to assess population abundances of relatively rare and delicate ciliated protists. These samples were taken directly into the sample bottle containing the fixative (5% final concentration by volume), and they were stored in the dark until analysis. For analysis, 100 ml subsamples were settled in Utermöhl chambers, and the cells were enumerated and measured at x400 with a Zeiss inverted microscope.

Cellular carbon contents of most autotrophic and heterotrophic taxa were estimated from cellular biovolumes (BVs, μm^3) following the modified *Strathmann* [1967] equations of *Eppley et al.* [1970]: $\log_{10}C = 0.94(\log_{10}BV - 0.60)$ for nondiatoms and $\log_{10}C = 0.76(\log_{10}BV - 0.352)$ for diatoms. For ciliates we converted BVs to carbon equivalents using a mean factor of 190 fg C μm^{-3} for Lugol's preserved cells [*Putt and Stoecker*, 1989].

2.4. HPLC Pigments

Seawater samples (~1.8 L) for pigment analyses were concentrated onto 25 mm Whatman GF/F glass fiber filters. The filters were wrapped in aluminum foil, immediately frozen in liquid nitrogen and stored at -85°C until analysis. Pigments were extracted in 100% acetone in the dark at 0°C for 24 hours, following disruption of the cells by sonication. Canthaxanthin (50 μL in acetone) was added as an internal standard in all samples. Prior to analysis the pigment extracts were vortexed and centrifuged to remove cellular debris.

Subsamples of 200 μL of a mixture of 1.0 mL pigment extract plus 0.3 mL H_2O were injected into a Varian 9012 HPLC system equipped with Varian 9300 autosampler, a Timberline column heater (26°C), and Spherisorb 5 μm ODS2 analytical column (4.6 X 250 mm) and corresponding guard

Table 2. Estimates of Phytoplankton Growth (μ_o, d^{-1}) and Microzooplankton Grazing (m, d^{-1}) Rates from Dilution Experiments Conducted on AESOPS Survey 1.[a]

Station	Z	% I_o	Chl_o	Chlorophyll a		Fucoxanthin		Total Cells	
				μ_o	m	μ_o	m	μ_o	m
1	35	23	241	0.17	0.14	0.31	0.11	0.35	0.14
1	55	10	227	0.23	0.14	0.26	0.05	0.27	0.11
8	45	10	313	0.20	0.20	0.24	0.21	0.30	0.23
12	32	23	250	0.30	0 15	0.26	0.06	0.16	0.15
12	49	10	206	0.22	0.14	0.28	0.13	0.18	0.03
18	25	23	235	0.21	0.17	0.26	0.09	0.17	0.01
18	45	10	256	0.25	0.23	0.32	0.18	0.23	0.11
23	18	23	859	0.08	0.13	0.18	0.10	0.02	0.18
23	28	10	903	0.10	0.10	0.09	0.07	0.22	0.10

[a]Z = depth (m) of water collection, % I_o = incubation light level as percent of incident surface PAR, and Chl_o = initial Chl a (ng L^{-1}). Rate estimates are based on Chl a and fucoxanthin (diatoms) from HPLC pigments and total phytoplankton cells from flow cytometry.

cartridge. Pigments were detected with a ThermoSeparation products UV2000 absorbance (436 nm) detector and analyzed according to *Andersen et al.* [1998]. Separations followed a modified ternary solvent protocol [*Wright et al.*, 1991], where eluent A is a 80:20 mixture of methanol:0.5 M ammonium acetate with 0.01% 2,6-di-tert-butyl-p-cresol; eluent B is a 80:15 mixture of acetonitrile:water; and eluent C is ethyl acetate. The linear gradient was 0' (90%A, 10%B), 1' (100%B), 11' (78%B, 22%C), 27.5' (10%B, 90%C), 29' (100%B), and 23' (100%B). Peak identifications were made by comparing the retention times of eluting peaks with those of pure standards and extracts prepared from algal cultures of known pigment composition [*Latasa et al.*, 1996]. Pigment concentrations (ng L^{-1}) were calculated using external and internal standards [*Bidigare*, 1991].

2.5. Experimental Rate Estimates

Dilution experiments were prepared similarly to *Landry et al.* [1995, 1998]. All experimental containers and transfer tubing (silicone) were precleaned with a modified *Fitzwater et al.* [1982] protocol. The items were soaked between uses in 10% trace metal grade HCl-milli-Q water and rinsed three times with freshly collected seawater prior to use. Plastic gloves were worn during all phases of experimental setup, subsampling and cleaning. For experiments at stations 1, 8, and 12, seawater was collected in 30 L, Teflon-lined Go-Flo bottles on a trace metal clean CTD rosette. After the trace metal rosette was lost during sampling operations, the regular CTD rosette with 10 L Niskin bottles was used for subsequent experiments. The switch in collection gear is presumed to have no impact on the rate determinations as direct comparisons of dissolved iron concentrations between Go-Flo (0.26 ± 0.03 nM, n = 5) and Niskin (0.23 ± 0.02 nM, n = 5) bottles at station 12 showed no difference [*Measures and Vink*, 2001]. The depths of water collection corresponded to the depths of penetration of ~10 and 23% of surface PAR as defined by the light extinction characteristics at each station (Table 2). Filtered water was obtained by direct gravity flow from the water bottles through an in-line filter capsule (Gelman Criticap 100, 0.2 μm pore size, presoaked for 1 hour in 10% HCl) to a clean polycarbonate carboy.

Ten 2.1 L polycarbonate bottles were used to establish a nutrient-enriched dilution series consisting of replicated bottles with 22, 45, 65, 86, and 100% natural (unfiltered) seawater. The filtered water was added first to the experimental bottles in measured amounts; then the bottles were gently filled and mixed with unfiltered seawater from the same depth. To promote constant phytoplankton growth in the dilution series, each bottle received added nutrients (final concentrations of 0.5 μM ammonium, 0.03 μM phosphate, 1.0 nM $FeSO_4$, and 0.1 nM $MnSO_4$). Five experimental bottles were filled with whole seawater without nutrient enrichment. Two of these were sacrificed for initial samples, and the final three were incubated as natural seawater controls. One additional bottle was filled with filtered seawater and run as a control to account for organisms that passed through the filter [*Li*, 1990]. All bottles were tightly capped after filling and incubated for 48 hours in seawater-cooled shipboard incubators constructed of light blue (color 2069) or dark blue (color 2424) Plexiglas with additional neutral density Plexiglas inserts to achieve the 23 and 10% light levels, respectively. The water-filled incubators were calibrated to incident PAR on site using a Biospherical QSL-100 quantum scalar irradiance meter.

HPLC pigment concentrations and FCM phytoplankton abundances were determined from measured concentrations in the initial bottles, the filtered water carboy, and the volumes of natural and filtered water in the dilution mixtures. Net rates of change (k, d^{-1}) were determined for each experimental treatment. Linear regressions of net growth rate against dilution factor (D_i is the proportion of natural seawater in the dilution treatment) for the nutrient-enriched treatments yielded estimates of phytoplankton growth (μ_n, growth with nutrients is the y-axis intercept) and phytoplankton mortality due to microzooplankton grazing (m is the regression slope). Phytoplankton growth without added nutrients (μ_O) was computed from the sum of grazing mortality m and mean net growth rate k_O in the unamended seawater treatments (i.e., $\mu_O = k_O + m$).

Instantaneous rates of phytoplankton community growth and grazing mortality were used to compute phytoplankton biomass production (PP, μg C L^{-1} d^{-1}) and grazing losses (G, μg C L^{-1} d^{-1}) according to the following equations [*Landry and Hassett*, 1982; *Landry et al.*, 2000; *Frost*, 1972]:

$$PP = \mu_o C_m,$$

$$G = mC_m,$$

$$C_m = C_{phyto}\,[e^{(\mu-m)t} - 1] / (\mu_o - m)t,$$

where C_m is the geometric mean concentration of phytoplankton carbon during the experiment and C_{phyto} is the initial phytoplankton carbon biomass determined from microscopical analyses. Since our μ and m estimates for these calculations were based on Chl a, the phytoplankton C:Chl a ratio is implicitly assumed to remain constant during the incubation. Biomass specific grazing estimates were determined by regressing (model II, reduced major axis) the rate of grazing mortality in each bottle ($m_i = \mu - k_i$) against microzooplankton biomass ($C_{\mu z,i} = D_i C_{\mu z,\,initial}$), where $C_{\mu z,\,initial}$ is initial carbon biomass from microscopical analysis.

2.6. Bio-optical Drifters

Eight METOCEAN Data Systems bio-optical drifters were deployed near the PF during the Survey I cruise (Table 3). The first cluster was deployed from November 8 to 9 1997, approximately along 171°W between 60.5° and 61°S. The second cluster, designed to estimate the horizontal vorticity field, was deployed on November 16 in a grid from 169.25° to 170°W and 60.5° to 60.9°S. The drifters were designed as discussed by *Abbott and Letelier* [1998] and drogued at 15 m to follow upper ocean currents. World Ocean Circulation Experiment (WOCE) Surface Velocity Program (SVP) drifters were also deployed at the same time as the bio-optical drifters. Although the SVP drifters had a shorter, wider drogue than the bio-optical drifters, the general patterns of circulation were similar between the two types.

Each drifter was equipped with optical sensors that measured upwelling radiance at 412, 443, 490, 510, 555, 670, and 683 nm and downwelling irradiance at 490 nm (E_d490). The sensors were mounted in the surface float, and data were relayed via Argos Data and Location System (ARGOS). The bio-optical data as well as sea surface temperature, drifter

Table 3. Release Dates (UT) and Locations, Initial Values of Temperature (°C) and Chl *a* (ng L^{-1}), and Mean Net Rates of Chl *a* Growth (μ_{net}, d^{-1}) for Instrumented Drifters Released in the PF During November 1997.[a]

Drifter	Date	Location	*T*, °C	Chl a	μ_{net}	*R*
52	Nov. 8	60.8°S, 170.8°W	1.59	244	0.027	0.97
49	Nov. 8	60.9°S, 170.9°W	1.85	263	0.025	0.97
51	Nov. 8	61.0°S, 170.8°W	-0.01	281	0.029	0.96
54	Nov. 11	61.1°S, 170.7°W	-0.24	281	0.024	0.86
48	Nov. 16	60.7°S, 169.7°W	1.36	343	0.034	0.91
53	Nov. 16	60.8°S, 169.9°W	1.09	322	0.030	0.95
21	Nov. 16	60.5°S, 169.2°W	0.59	363	0.011	0.72
47	Nov. 16	60.6°S, 169.3°W	-0.027	316	0.016	0.72

[a]Temperature and Chl *a* are means of the first five data records from each drifter. Net growth rates were determined from exponential fits of average daily Chl *a* versus Year Day for all observation days in November; *R* is the correlation coefficient. Data are in order of day of drifter release.

position and other data were processed following the methods of *Abbott and Letelier* [1998]. The Chl *a* concentrations were estimated from the ratios of measured irradiances at 443 and 555 nm [*Clark*, 1981] using calibration parameters for Southern Ocean surface waters [*Letelier et al.*, 1997].

3. Results

3.1. Water Column Properties

The five intensively sampled stations fall into three groups based on measured hydrographic parameters (Table 1). Station 1 (57°S) was substantially north of the PF, with relatively warm water temperature (4°C) and lower concentrations of major nutrients (23, 1.6 and 8.3 μM for N, P, and Si, respectively) than the other stations. As determined by sea surface temperature [*Barth et al.*, 2001], stations 8 and 23 were on the southern edge of the frontal jet with nearly identical low temperature (0°C) and higher nutrients (28, 2, and 26 μM N, P, and Si). Stations 12 and 18 were on the northern side of the front, with intermediate mixed layer temperatures (1.8°-2°C) and nutrient concentrations (27, 1.8, and 15-17 μM, respectively). Mixed layer salinities showed only a slight decrease from north to south among the five stations, reflecting relatively little influence of sea ice melt.

Mixed layer depths (MLD) differed also among stations (Table 1), but their variations followed more of a temporal trend, particularly when viewed in the context of other cruise observations (Figure 1). Because density gradients were often relatively small in the upper water column, MLD varied appreciably with definition. By more stringent definition, for example, a 0.05 kg m^{-3} increase in sigma t over surface values, MLD was only rarely shallower than 200 m and sometimes as deep as 300 m. By more relaxed definition (e.g., Δ = 0.01 or 0.005 kg m^{-3}) the gradual shoaling of MLD from 170-200 m initially to <100 m is apparent. Even within this general trend, however, profiles taken close together in time but at different positions in the frontal system (e.g., SeaSoar profiles to >300 m at ~7 min intervals) exhibited considerable variability (Figure 1). For the purposes of the present study, the shoaling of MLD appeared to be particularly notable for waters on the northern edge of the frontal jet during SeaSoar sampling from YD 311 to 317, but the details of these results and their implications are presented elsewhere [*Barth et al.*, 2001].

Euphotic zone depth (EZD), defined as the depth of penetration of 1% of incident PAR from CTD depth profiles, varied narrowly between 91 and 98 m at the first four sampling stations but was shallower (62 m) at station 23 because of the higher concentration of phytoplankton (Figure 1). When the measurements overlapped, the pattern of daily integrated short-wave radiation corresponded closely to the

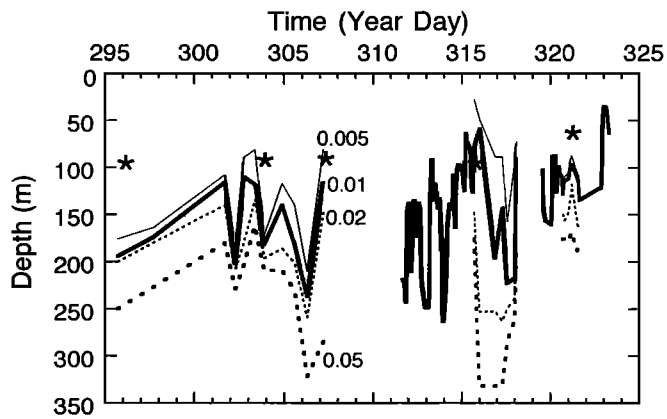

Figure 1. Estimates of MLD during AESOPS Survey I according to different criteria (depth at which there is a 0.005, 0.01, 0.02, or 0.05 kg m^{-3} increase in σ_T density relative to near-surface waters). The four MLD estimates are given for each hydrographic station at which they were assessed from CTD profiles. Heavy solid line emphasizes Δ 0.01 kg m^{-3} criteria, which was also assessed at hourly averaged frequency during SeaSoar mapping activities (e.g., days 311-315, 319-320, and 321-323). Star symbols give euphotic zone estimates (penetration depths of 1% incident solar radiation) at the five experimental stations. SeaSoar estimates courtesy of T. Cowles and J. Barth, Oregon State University

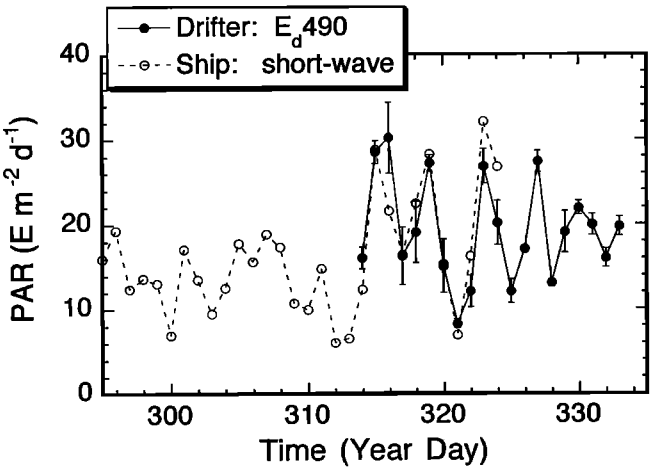

Figure 2. Estimates of PAR during AESOPS Survey I. Daily integrated values are the means from surface drifters (solid symbols; error bars are standard deviations) measured as downwelling irradiance at 490 nm (E_d490) and from ship-measured long-wave radiation corrected for the mean ratio of short-wave to E_d490 during the time when both measures overlapped. PAR estimates are computed from E_d490 as described in text.

pattern of E_d490 downwelling irradiance (Figure 2). PAR estimates derived from the blended E_d490 and short-wave light records show a substantial difference between mean light conditions for the first and second halves of the cruise. In particular, surface incident solar radiation increased fivefold from cruise low values on YD 312 to cruise high levels on YD 315 and 316. During this time, SeaSoar mapping showed a marked shoaling of the mixed layer (Figure 1).

3.2. Phytoplankton Abundance and Biomass

Despite the expectation that microscopy and FCM analyses with different sensitivity ranges and thresholds would reveal different components of the autotrophic community we found surprising agreement among population estimates for the three methods (Figure 3). The agreement in total abundance estimates was particularly striking for station 1, and only at station 18 did they appear to be consistently offset. Among all stations, however, the results do not suggest systematic differences among methods. Thus, on the basis of several lines of evidence, phytoplankton cell abundances were highest at station 1 (~6000 cells mL^{-1}), lowest at station 23 (2000-3000 cells mL^{-1}), and intermediate at stations 8, 12 and 18 (3000 - 6000 cells mL^{-1})

One important difference among analytical methods was the precision of the abundance estimates. Using all samples collected in the upper 70 m as "replicate observations," the mean coefficient of variation for microscopical estimates was 20% of the sample mean, while the mean precision of FCM analyses were 10 and 3% of the means for SV and LV samples, respectively. Given the good sampling statistics for FCM analyses, the abundance and cellular fluorescence profiles from such analyses provide relatively sensitive indices of the (biological) stratification of the water column from the perspective of phytoplankton cells. For instance, even within the depths that appear to be well mixed from physical criteria, gradients in phytoplankton abundance were evident, with higher concentrations closer to the surface (Figure 3). Most fluorescence profiles also showed reduced pigmentation per cell near the surface (Figure 4), particularly at stations 8 and 23, indicating that the cells had resided there sufficently long to photo-adapt relative to others deeper in the "mixed" layer. In addition, the depths at which changes appear to occur in abundance or fluorescence profiles suggest, to varying degrees, biological divisions in the water column from 160 to 200 m at station 1, 130 to 150 m at station 12, 50 to 100 m at station 18, and 50 to 70 m at station 23. These depths conform more closely to the less stringent physical definitions of the mixed layer (Δ 0.01 or 0.005 kg m^{-3}); thus these definitions appear to be the most relevant for biological interpretations.

The biomass structure and composition of the plankton community tend to follow the three station groupings based

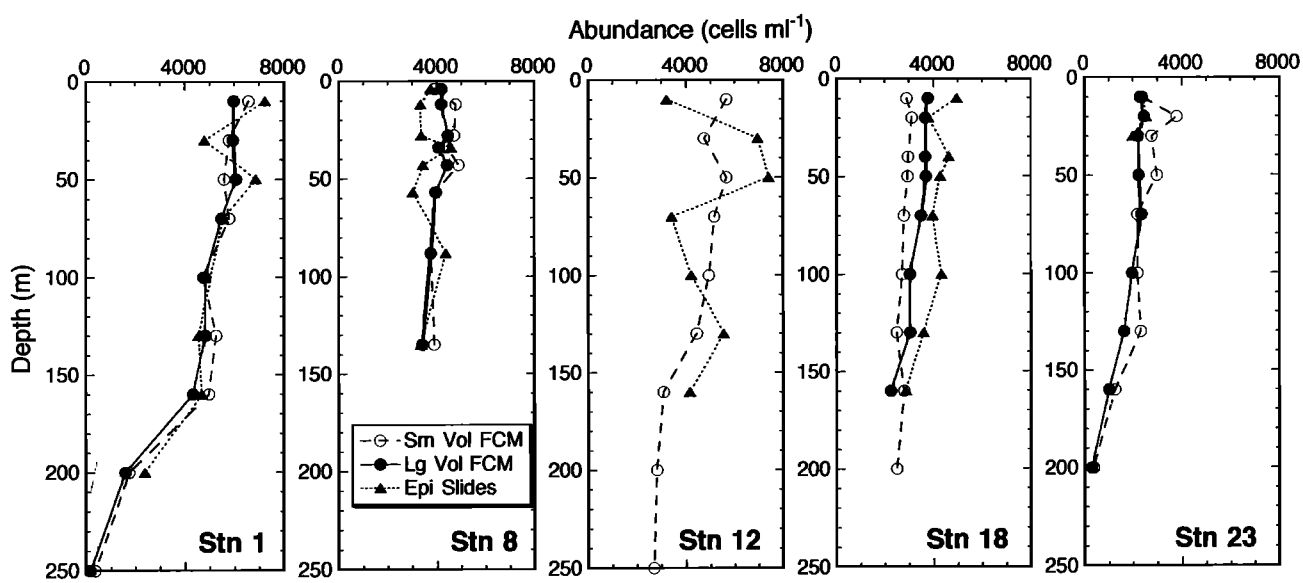

Figure 3. Station depth profiles of phytoplankton abundance based on cell counts from SV and LV flow FCM and epifluorescence microscopy. LV FCM data are not available for station 12.

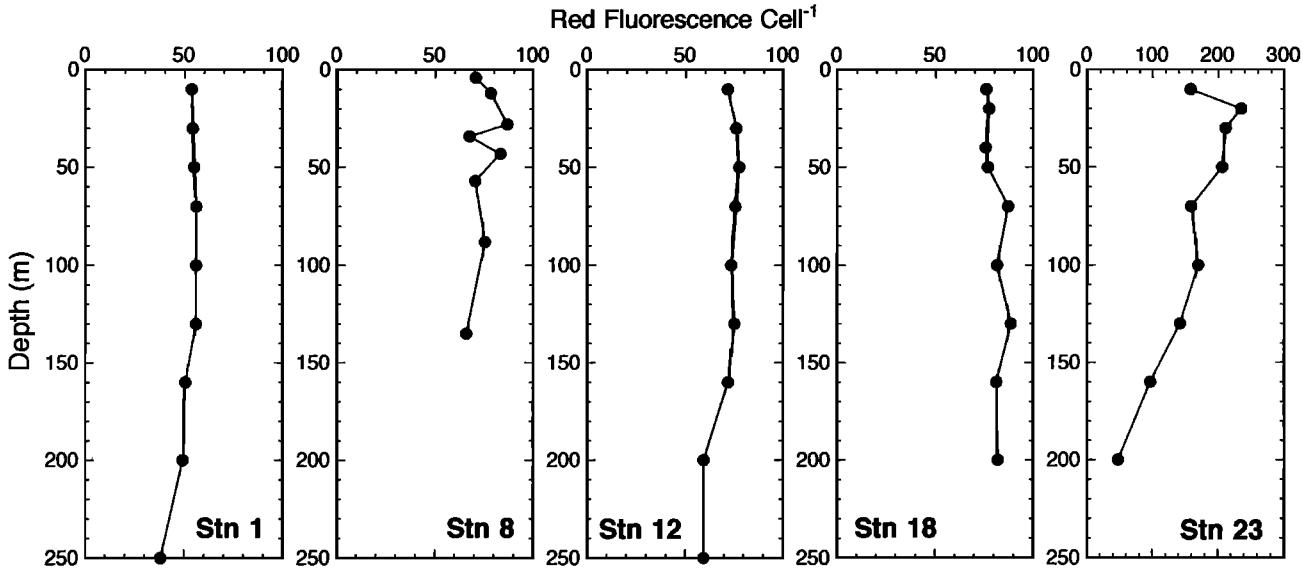

Figure 4. Station depth profiles of phytoplankton mean cellular red fluorescence based on SV FCM analyses.

on physical and chemical properties (Figure 5). Stations 8 and 23 stand out as having a structure skewed toward larger (>20 μm) phytoplankton, with a relatively high complement of diatoms. The peak in 5-10 μm cells at station 23 was principally *Phaeocystis* cells in colonial form; thus, with respect to availability to microherbivores, they functionally enhance the relative importance of large phytoplankton at this station. In comparison, stations 12 and 18 showed a more even size distribution of autotrophs and lower biomass of diatoms and ciliates. Although total autotrophic biomass was similar at station 1 to that at stations 12 and 18, larger cells, particularly diatoms, were rare. In addition, station 1 exhibited a higher standing stock of protistan grazers relative to autotrophic biomass than the other stations, and this excludes any contribution by ciliates as Lugol's samples were not taken at station 1.

3.3. Phytoplankton Growth and Microzooplankton Grazing

Phytoplankton growth rate estimates from dilution experiments ranged from 0.08 to 0.30 d^{-1} and averaged (± standard deviation) 0.20 ± 0.07 d^{-1} for chlorophyll-based community analyses (Table 2). Rate estimates based on fucoxanthin (FUCO), an assumed proxy for diatoms [*Bidigare*

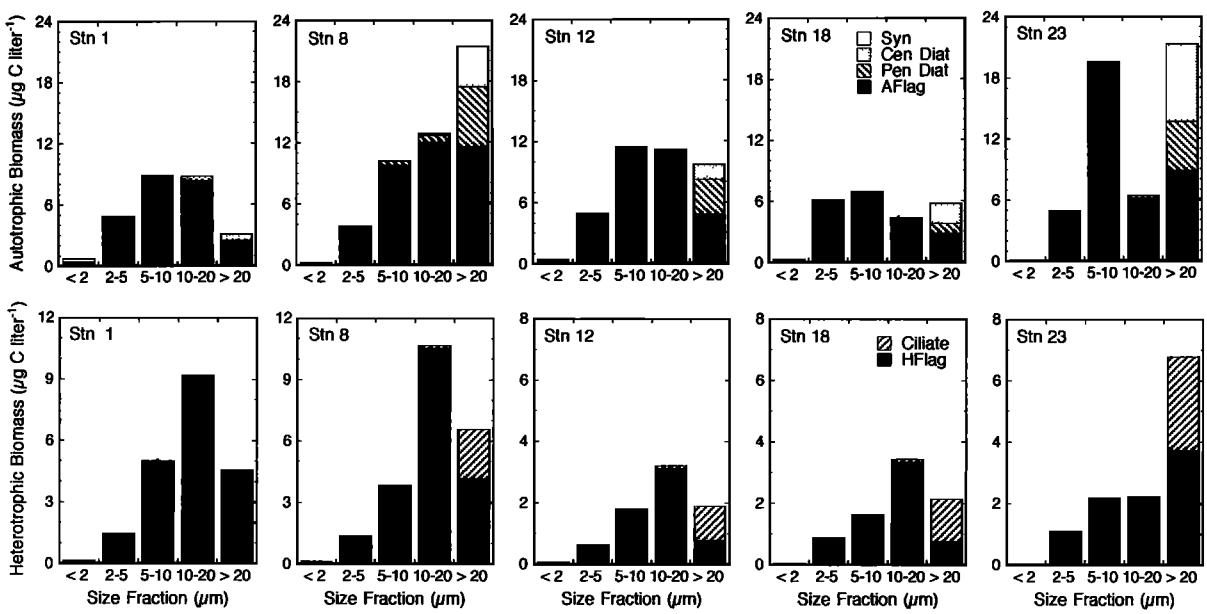

Figure 5. Biomass structure of autotrophic and heterotrophic protists at experimental stations. Size distributions are the means of microscopical biovolume-based carbon estimates for all mixed layer samples: Syn, *Synechococcus* spp.; Cen Diat, centric diatoms; Pen Diat, pennate diatoms; AFlag, autotrophic flagellates; and HFlag, heterotrophic flagellates.

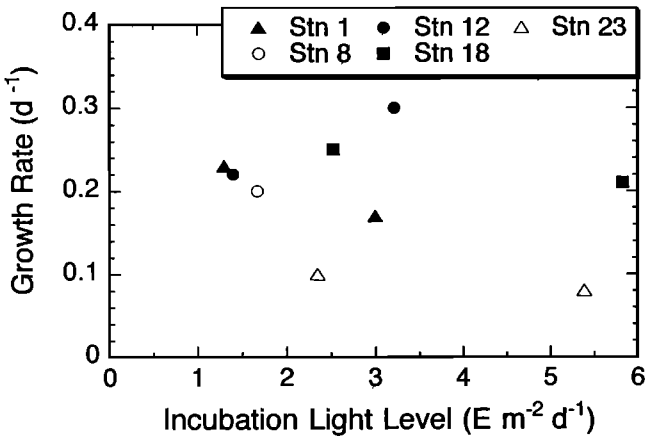

Figure 6. Effects of incubation light level on Chl *a* growth rates estimates from dilution experiments during October-November 1997. Mean light levels were calculated from the daily integrated estimates of PAR (Figure 2) during the two days of experimental incubations and the percent transmission of shipboard incubator boxes (10 or 23%; Table 2).

et al., 1996], were typically a little higher, averaging 0.24 ± 0.07 d^{-1}. Pigment-based growth estimates were similar to estimates based on FCM analyses of phytoplankton cells (0.21 ± 0.095 d^{-1}), implying relatively balanced cellular and pigment growth on average. Not surprising, however, given inherent methodological imprecisions, the rate agreement within individual experiments was variable. Cruise-averaged estimates of microzooplankton grazing were 0.16 ± 0.04, 0.11 ± 0.05, and 0.12 ± 0.07 d^{-1}, for Chl *a*, FUCO, and total cells, respectivley. Overall, the net growth rates of diatoms inferred from FUCO analyses (0.13 ± 0.07 d^{-1}) were substantially higher than community net growth estimates from Chl *a* (0.04 ± 0.06 d^{-1}) and total autotrophic cells (0.09 ± 0.11 d^{-1}).

Although the experimental data are limited and non-synoptic, the stations appear to divide into two groups on the basis of their growth and grazing characteristics. For stations north of the frontal jet (1, 12, and 18), mean growth rates were higher than stations (8 and 23) south of the jet. This was due to depressed growth estimates at station 23, which involved samples incubated during a period of pronounced increase in solar radiance (YD 321-323; Figure 2). Otherwise, growth rate estimates showed little influence of light level over the approximately fivefold range of incubation conditions (Figure 6).

Mean net community growth rates at the two southern stations were not significantly different from zero (-0.01 and 0.01 d^{-1} for Chl *a* and cells, respectively), but net rates at the northern stations were consistently positive (0.07 ± 0.05 and 0.14 ± 0.07 d^{-1}). These station groups also differed with respect to the biomass specific grazing impacts of their heterotrophic assemblages (Figure 7). For the northern stations (2°-4°C), phytoplankton grazing mortality increased 0.1 d^{-1} per 3.6-4.4 μg C L^{-1} increase in microheterotroph biomass. Approximately twice the heterotrophic biomass (8.3 μg C L^{-1}) was needed for a comparable mortality impact at the more southern stations (~ 0°C). For all stations, however, estimates of phytoplankton carbon consumption largely fell in the range of 40-100% of heterotrophic protist biomass per day with as much variability between experiments at a given station as between the north and south station groups (Figure 8).

3.4. Rate Estimates From Drifters

Figure 9 shows the paths of instrumented drifters from day of release through the first week of December. West of about 168.5°W, all drifters followed relatively coherent streamlines to the NE and over a PF meander. Thereafter, the paths diverged, with those on the northern side of the jet flowing north and those on the southern side turning to the south. For frame of reference, stations 8 and 23 were at locations that should have followed the southerly path, and station 18 was in the path of drifters that turned north. Station 1 and 12 were out of the area where released drifters defined the flow field. Sea surface temperature measured by the drifters increased during November at an average rate of 0.05°C d^{-1}, with little

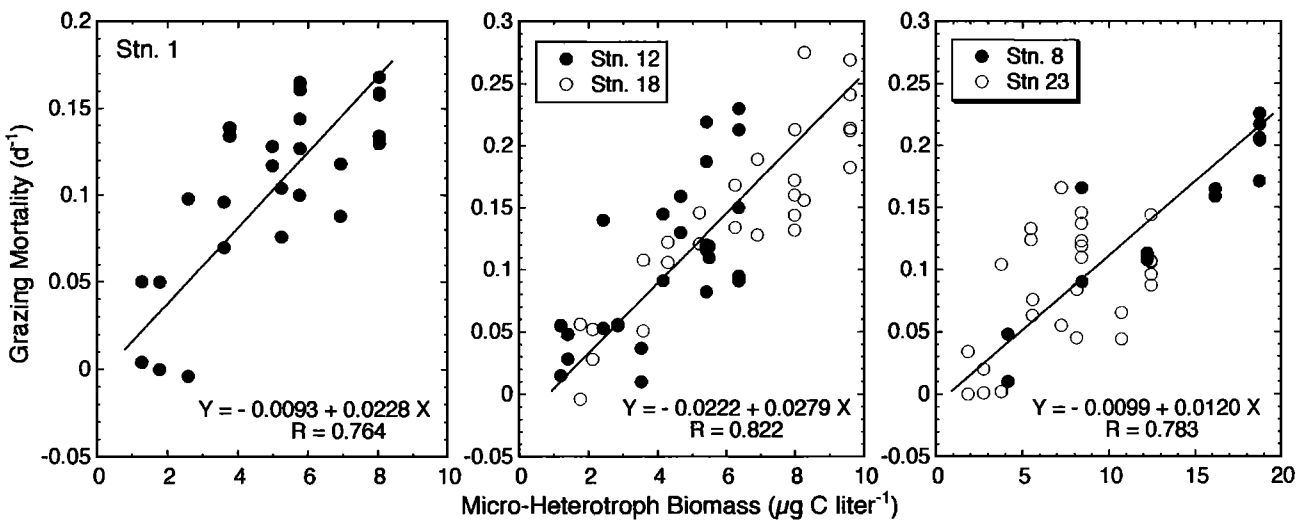

Figure 7. Relationships between microherbivore grazing impact on phytoplankton and grazer biomass in dilution experiments conducted during AESOPS Survey I. Equations are from model II (reduced major axis) linear regressions.

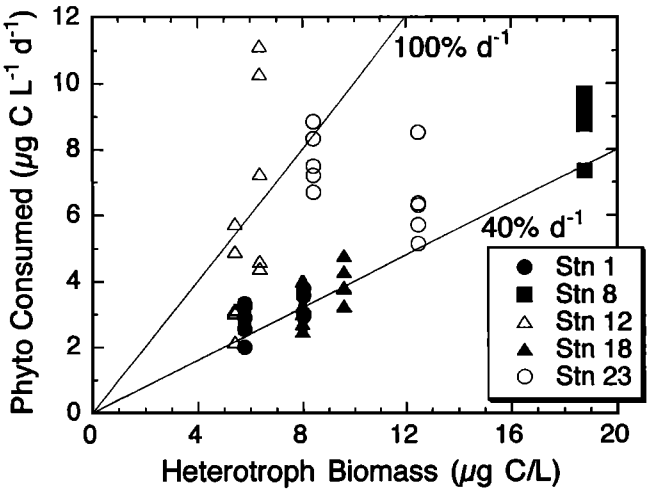

Figure 8. Phytoplankton carbon consumption by heterotrophic protists in dilution experiments conducted during AESOPS Survey I. Lines indicate biomass specific rates of 40 and 100% of grazer carbon per day.

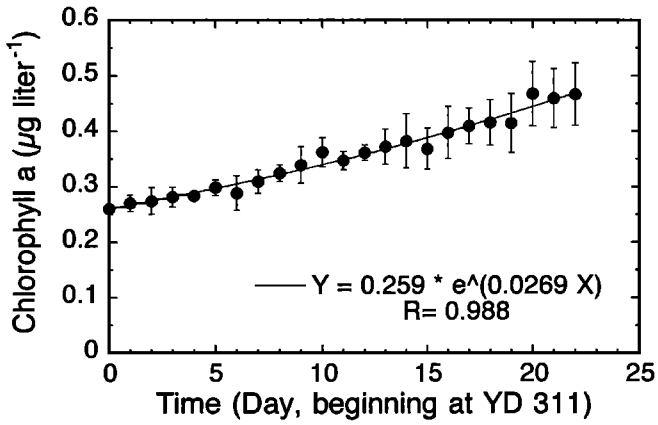

Figure 10. Mean daily estimates of phytoplankton Chl *a* (± standard deviation) from drifters released in the Antarctic PF during AESOPS Survey I. Mean net growth rate (0.027 d^{-1}) is estimated from the best fit of an exponential growth model to the observed Chl *a* increase.

distinction among drifters released at different times, at different initial temperatures, or following different paths.

On the basis of mean daily Chl *a* estimates from all drifters the net growth of phytoplankton through the month of November was well described by a constant exponential rate of 0.027 d^{-1} (Figure 10). Individually, net growth rates for six of the drifters (0.024-0.034 d^{-1}) were within ±25% of the mean estimate (Table 3). However, the other two drifters (21 and 47), both released south of the jet and late in the cruise, showed substantially lower net growth (0.011 and 0.016 d^{-1}, respectively). Variability in daily estimates of net Chl *a* for each drifter was substantial, ranging from -0.1 to 0.3 d^{-1} (Figure 11). The two drifters released early on the northern side of the frontal jet (49 and 52) showed no relationship between net growth and maximum daily irradiance (as measured from the drifter close to local noon). For the other drifters (excluding 54 because of its spotty record) the relationship was negative, implying that any growth increase on bright days (or decrease on dark days) was more than offset by the opposite trend in photoacclimation of cellular Chl *a* content.

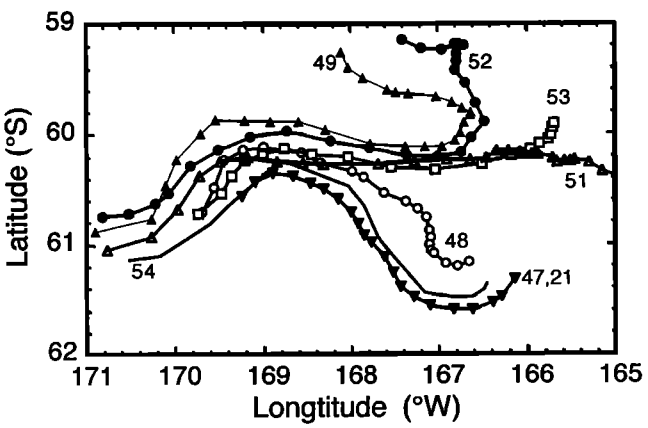

Figure 9. Flow paths for instrumented drifters released in the Antarctic PF during AESOPS Survey I. Symbols are daily increments from positions at approximately midday (UT) from day of release through day 339 (early December 1997). Sporatic data transmission from drifter 54 precluded accurate representation of its daily position.

4. Discussion

4.1. Phytoplankton Growth Conditions in the PF

The seasonal timing of the present study was similar to that of the JGOFS ANT X/6 cruise (R/V *Polarstern*, October 2 to November 25 1992), during which German and Dutch scientists explored the spring phytoplankton increase in the PF (47°-50°S, 0-10°W) north of the Weddell Sea. The observations at the two sites provide an interesting contrast in phytoplankton growth conditions in the Atlantic and Pacific sectors of the PF. In the Atlantic the PF lies directly downstream of the Drake Passage and in the wake of the south Sandwich Islands [*Smetacek et al.*, 1997; *Veth et al.*, 1997]. Proximity to land masses and margin sediments enhances iron concentrations in the polar jet [*Löscher et al.*, 1997], leading to substantial accumulations of phytoplankton biomass and bloom concentrations of large diatoms [*Bathmann et al.*, 1997; *Crawford et al.*, 1997; *Detmer and Bathmann*, 1997]. Possibly also as a consequence of the lower latitude of the Atlantic PF and its implications for higher light and surface temperature (3°-4°C), the spring phytoplankton increase appears to begin relatively early. During the first occupation of the PF stations on the ANT X/6 cruise (October 17-19, 1992; YD 290-292), Chl *a* concentrations (~ 0.7 μg L^{-1}) were already higher than those recorded throughout the month of November by drifters released in the present study (Figure 10). Later during ANT X/6 (November 10-21), Chl *a* concentrations as high as 4 mg m^{-3} were measured, with a mean concentration of about 2 μg L^{-1} broadly distributed between 47° and 50°S [*Bathmann et al.*, 1997]. Concentrations of about 1 μg Chl *a* L^{-1} were observed late in the present study only in a mesoscale feature south of the polar jet [*Barth et al.*, 2001; *Brown and Landry*, 2001], the border of which was sampled at station 23 (Table 2). Otherwise, concentrations approaching those observed during ANT X/6 were not measured in or close to the PF at

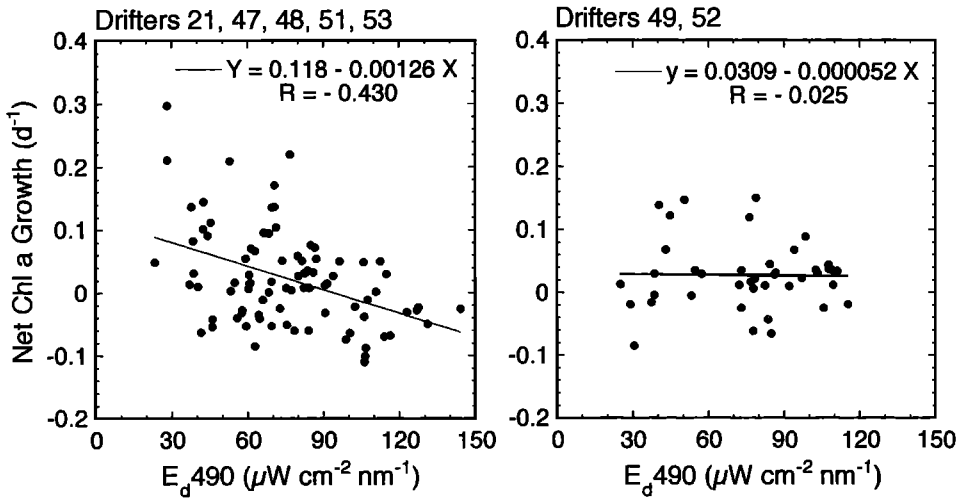

Figure 11. Relationship between daily estimates of Chl *a* growth for individual drifters and downwelling irradiance at 490 nm measured at the same drifter during peak daylight hours (local midday).

170°W at any time during austral summer 1997 [Landry et al., Seasonal dynamics of phytoplankton in the Antarctic Polar Front Region at 170°W, submitted to *Deep-Sea Research*, 2000].

The observed differences in magnitudes of phytoplankton standing stocks in the Atlantic and Pacific PF studies are consistent with different rates of supply and availability of iron. We can also infer from the relative scarcity of large bloom-forming diatoms (e.g., *Fragilariopsis* and *Corethron* spp.) in the PF at 170°W that the growth rates of at least some components of the plankton community must be strongly affected by the lower iron concentrations there. The situation is less clear for the dominant small phytoplankton, which may be growing at close to their physiological maximum rates, even if these are somewhat lower than the potential rates of large diatoms under iron replete conditions [e.g., *Eppley*, 1972; *Scharek et al.*, 1997]. Certainly, one could argue that growth rates are less likely to be held below physiological "potential" by iron in spring versus summer seasons because the deeper springtime mixing brings more iron into surface water and because the growth potential is set lower by temperature and light. Our bottle growth estimates of 0.2-0.3 d^{-1} correspond to population doubling times of 2.3-3.5 days and vastly exceed the rate at which phytoplankton biomass accumulates in the environment. Thus the relevant growth issue is not so much that these rates could be even higher but why the observed rate of increase is so slow.

As a first step to resolving this issue, we should ask how observed variability in the mixed layers during the Survey I cruise will affect our interpretations of rate estimates from bottles incubated at fixed percentages of incident solar radiation. For this we assume a fixed depth of 95 m for 1% penetration of PAR (Figure 1), and therefore a mean extinction coefficient k_z of 0.048 m^{-1}. Under these conditions the mean light level in a mixed layer of 100 m would be 20.7% of incident PAR. Phytoplankton in fully mixed layers of 200 and 300 m depth would likewise experience average light levels of 10.4 and 6.9% of surface PAR, respectively. Other factors (spectral quality and solar angle) would need to be considered if we were to compare light conditions in the water column and the shipboard incubators more precisely. As a first approximation, however, our fixed 10 and 23% light levels would seem to fit reasonably well the mean light levels expected for phytoplankton mixed to at least twice the depth of the classically defined euphotic zone. Given the lack of consistent differences in the rate estimates from the two light levels (Figure 6), one might also conclude that they are above the light level at which growth response declines linearly with light dose. Therefore the averaged rates for these experiments presumably apply to mixed layers in which the mean light conditions are saturating for cell growth.

In terms of actual incubator light levels, growth rates > 0.2 d^{-1} were achieved in our experiments at irradiance estimates as low as 1.2 E m^{-2} d^{-1} (= 14 μE m^{-2} s^{-1}) (Figure 6). This is substantially lower than the "net photocompensation irradiance" (35 μE m^{-2} s^{-1}) assumed in *Nelson and Smith*'s [1991] calculations of critical depth in the Southern Ocean. *Nelson and Smith* [1991] noted that their estimate came from the Gulf of Maine and was likely [*Nelson and Smith*, 1991, p.1653] "the greatest source of uncertainty" in their computations. According to the present results, the PF phytoplankton community appears to be particularly well adapted to grow and function at low light levels during springtime. Compensation irradiance estimates of $\leq$10 μE m^{-2} s^{-1} may be appropriate for assessing their production responses according to critical depth theory.

On the basis of biological indices of phytoplankton stratification (cell abundance or chlorophyll fluorescence) a weak physical gradient often separates a light sufficient component of the community from one residing entirely below the euphotic zone (e.g., Figures 3 and 4). These density gradients are assumed to break down occasionally, if not frequently, under strong wind forcing during the early spring, effectively spreading the net phytoplankton growth achieved in the upper layer over a broader depth range and resetting near-surface concentration to a lower depth-averaged level. The partitioning of the upper water column into two zones, one of which contains the full complement of growing phytoplankton and grazing protists and the other with grazers but insufficient light for phytoplankton growth, needs to be considered in the interpretation of growth and grazing rates from dilution experiments. Any net growth implied in

experimental results (Table 2) applies only to the upper layer and may be offset by additional grazing losses below the euphotic zone.

As reviewed by *Banse* [1996], the classic prerequisites for high-latitude phytoplankton blooms, a shoaling mixed layer and seasonally increasing light, fail to explain large parts of the Southern Ocean, where iron regulates the growth of large phytoplankton and protists consume most small cells produced. Indeed, beyond the lower temperature-dependent rates, there is little to distinguish experimental results in the PF at 170°W from those from more extensively studied high nutrient-low chlorophyll regions in the subarctic and equatorial Pacific [e.g., *Miller et al.*, 1991; *Price et al.*, 1994; *Landry et al.*, 1997]. In all high nutrient-low chlorophyll studies to date, high microzooplankton grazing activity dominates the phytoplankton loss processes, balancing, or nearly balancing, relatively high rates of phytoplankton growth [e.g., *Strom and Welschmeyer*, 1991; *Landry et al.*, 1993, 1995]. In the present study, for example, microzooplankton grazing consumed on average only 14% of Chl *a* standing stock per day but consumed 79% of daily production.

The small net growth estimate from bottle incubations (0.04 d^{-1}) ordinarily would be assumed to be lost to other processes (e.g., sinking or mesozooplankton grazing) not measured in the bottles. In the present case, however, the relatively close agreement between net rates observed in bottles and those measured by instrumented drifters (0.03 d^{-1}) would seem to imply that these other loss processes were small, on average, at the stations and times examined. This impression is somewhat contradicted by experimental analyses based on FUCO and total cells, in which grazing accounts for only 46 and 57%, respectively, of phytoplankton growth. Part of the higher net growth of total cells might be explained by the ability of the flow cytometer to recognize ingested cells as "autotrophic" from their residual phaeopigment content. Thus FCM cell analysis may tend to underestimate true grazing rates. On the other hand, diatoms represent a relatively small fraction of the total community that could well be growing at higher than average rates, suffering reduced grazing to protozoans, and ultimately losing more to sinking and mesozooplankton grazing in the natural environment. Relatively high growth rates of diatoms are a common observation in incubation experiments from HNLC regions [e.g., *Strom and Welschmeyer*, 1991; *Landry et al.*, 1993; *Fryxell and Kaczmarska*, 1994; *Latasa et al.*, 1997]. These are typically not large bloom-forming diatoms but rather species with slender elongated shapes, large internal vacuoles and high surface area:volume ratios that may function as small cells with respect to the uptake of limiting substrates [*Landry et al.*, 2000].

4.2. Temporal and Spatial Scales

As used in the present study, the traditional shipboard station approach offers many advantages in terms of intensive sampling and process-oriented experimental studies. However, its slow pace and spotty coverage are ill suited for resolving temporal and spatial dynamics in a complex region like the Antarctic PF. We are therefore fortunate in having additional observational strategies during the Survey I cruise, including instrumented drifters, Sea Soar maps and occasional glimpses of the area by satellite, to help place our limited results in a broader context.

First, it is evident from semisynoptic mapping surveys [*Barth et al.*, this issue] that the elevated Chl *a* and phytoplankton biomass at station 23 at the end of the cruise was a local enhancement associated with a frontal jet meander rather than a dramatic blooming of the whole study area. SeaSoar observations suggest that this feature originated from upstream steaks of higher Chl *a*, likely representing localized zones of upwelling and enhanced phytoplankton growth stretched into coherent streamlines by current shear. Among the stations sampled, *T-S* properties of the water at station 8 were closest to those in the developing bloom [*Barth et al.*, this issue]. Nonetheless, it is unclear whether the experimental results from this or any other sampling station truly reflect the growth potential of phytoplankton that ultimately comprise the meander feature. Station 8 might just as easily have sampled conditions in the less productive bands between streaks or some intermediate condition.

Streamline analysis of chlorophyll in the SeaSoar maps indicate that rates of 0.05 ± 0.01 d^{-1} can account for in situ growth of phytoplankton leading to the meander feature [*Barth et al.*, this issue; *Brown and Landry*, this issue]. At first glance this is encouragingly close to, and statistically no different than, the mean net growth rate (0.04 ± 0.06 d^{-1}) measured experimentally. We are cautious, however, in taking the individual experimental results at face value. One indication of potential problems in this regard is the failure of experimental estimates to predict correctly where in the PF region that significant net growth of phytoplankton would occur. Incubation experiments suggested that the northern and warmer side of the PF jet should have had the highest net growth (Table 2); observations indicated that the accumulation occurred in colder water on the southern side. This discrepancy could be the result of photoadaptive effects during experimental incubations. By coincidence, experiments at stations on the southern side (stations 8 and 23) were both conducted during periods of significant increasing trends in downwelling radiation, which would have led to pigment-based underestimates of true growth rates. Conversely, two of the three periods during which experiments from the northern stations (stations 1 and 12) were conducted coincided with times of declining downwelling radiation. Pigment photoadaptation during these experiments would have been expected to exaggerate slightly the growth rates from these stations. Clearly, the magnitude of ecologically meaningful net growth rates in this region is very small, and their measurements can be significantly affected by day-to-day variability in environmental (and experimental) circumstances. Resolving the true mean growth responses of different subregions within the PF Zone would require many more experiments that those presented here.

Pigment photoadaptation also likely explains the slight differences in estimates of net chlorophyll increases from surface drifters (0.03 d^{-1}) and SeaSoar maps (0.05 d^{-1}) [*Barth et al.*, this issue]. When drifters were released earlier in the cruise, under conditions of reduced downwelling radiation and deeper mixing, their estimates of Chl *a* concentration were in relatively good agreement with shipboard and SeaSoar assessments. Later in the cruise, when the drifters were advected through the region of enhanced pigment concentration, they measured roughly half (0.5 – 0.6 μg Chl *a* L^{-1}) of the concentrations observed in deeper profiles. The SeaSoar estimates of net growth rate were based on the

increase in depth-integrated Chl *a* to 300 m. SeaSoar vertical sections [e.g., *Barth et al.*, this issue, Plate 6] and the vertical profile of chlorophyll red fluorescence $cell^{-1}$ at station 23 provide strong evidence of depressed phytoplankton pigment in the layer sampled by drifters. Thus we conclude that the timescales of mixing later in the cruise were insufficient to override biological stratification of near-surface waters, evident as reduced Chl *a* $cell^{-1}$. This, in turn, caused the surface drifters to miss the true magnitude of the spring Chl *a* increase and underestimate the mean net rate of increase by about 0.02 d^{-1}. This is a relatively small error in absolute terms but is meaningful when extrapolated to standing stock increases over many days.

In summary, experimental rate measurements in the PF region at 170°W during the spring 1997 indicated an actively growing phytoplankton community. The mean specific rate of phytoplankton growth was slightly in excess of 0.2 d^{-1} and grazing to protistan consumers accounted for daily losses of 70-80% of primary production. The slow net rates of Chl *a* increase in experimental bottles (0.04 d^{-1}) were in good agreement with in situ accumulation rates determined from instrumented drifters (0.03 d^{-1}), but both may be slight underestimates of the actual increase in phytoplankton carbon due to pigment photoadaptive effects. Given these effects, the present results are consistent with the slightly higher net rates (~0.05 d^{-1}) determined from streamline analysis of SeaSoar chlorophyll maps and pigment-adjusted estimates of near-surface phytoplankton carbon, as described by *Barth et al.* [this issue] and *Brown and Landry* [this issue], repectively.

Acknowledgments. This study was supported by NSF grants OPP-9634053 (MRL) and –9530507 (MRA). We gratefully acknowledge the many shipmates and colleagues whose efforts facilitated and contributed to our results, particularly the captain and crew of the R/V *Roger Revelle*, the hydrographic team, lead by L. Codispoti, and Chief Scientist T. Cowles. We also thank J. Barth and T. Cowles for providing SeaSoar mixed layer estimates for Figure 1. This paper is contribution 661 from the U.S. JGOFS Program and 5429 from the School of Ocean and Earth Science and Technology, University of Hawaii at Manoa, Honolulu, Hawaii.

References

Abbott, M.R., and R.M. Letelier, Decorrelation scales of chlorophyll as observed from bio-optical drifters in the California Current, *Deep Sea Res., Part I, 45*, 1639-1668, 1998.

Abbott, M.R., J.G. Richman, R.M. Letelier, and J.S. Bartlett, The spring bloom in the Antarctic Polar Frontal Zone as observed from a mesoscale array of bio-optical sensors, *Deep Sea Res., Part II, 47*, 3285-3313, 2000.

Andersen, R.A., D. Potter, R.R. Bidigare, M. Latasa, K. Rowan, and C.J. O'Kelly, Characterization and phylogenetic position of the enigmatic golden alga *Phaeothamnion confervicola*: Ultrastructure, pigment composition and partial SSU rDNA sequence, *J. Phycol., 34*, 286-298, 1998.

Baker, K.S., and R. Frouin, Relation between photosynthetically available radiation and total insolation at the ocean surface under clear skies, *Limnol. Oceanogr., 32*, 1370-1377, 1987.

Banse, K., Low seasonality of low concentrations of surface chlorophyll in the Subantarctic water ring: Underwater irradiance, iron, or grazing?, *Prog. Oceanogr., 37*, 241-291, 1996.

Barth, J. A., T.J. Cowles, and S.D. Pierce, Mesoscale physical and bio-optical structure of the Antarctic Polar Front near 170°W during austral spring, *J. Geophys. Res.*, this issue.

Bathmann, U.V., R. Scharek, C. Klaas, C.D. Dubischar, and V. Smetacek, Spring development of phytoplankton biomass and composition in major water masses of the Atlantic sector of the Southern Ocean, *Deep Sea Res., Part II, 44*, 51-67, 1997.

Bidigare, R.R., Analysis of algal chlorophylls and carotenoids, *Marine Particles: Analysis and Characterization, Geophys. Monogr. Ser.*, vol. 63, edited by D.C. Hurd and D.W. Spencer, pp. 119-123, AGU, Washington, D. C., 1991.

Bidigare, R.R., J.L. Iriarte, S.-H. Kang, M.E. Ondrusek, D. Karentz, and G.A. Fryxell, Phytoplankton: Quantitative and qualitative assessments, *Foundations for Ecosystem Research in the Western Antarctic Peninsula Region, Antarctic Res. Ser.*, vol. 70, edited by R. Ross, E. Hoffman, and L. Quentin, pp. 173-198, AGU, Washington D. C., 1996.

Brown, S.L., and M.R. Landry, Mesoscale variability in biological community structure and biomass in the Antarctic Polar Front region at 170°W during austral spring 1997, *J. Geophys. Res.*, this issue.

Clark, D.K., 1981. Phytoplankton pigment algorithm for the Nimbus-7 CZCS, in *Oceanography from Space*, edited by J.F.R. Gower, pp. 227-238, Plenum, New York, 1981.

Crawford, R.M., F. Hinz, and T. Rynearson, Spatial and temporal distribution of assemblages of the diatom *Corethron criophilum* in the Polar Frontal region of the South Atlantic, *Deep Sea Res., Part II, 44*, 479-496, 1997.

Detmer, A.E., and U.V. Bathmann, Distribution patterns of autotrophic pico- and nanoplankton and their relative contribution to algal biomass during spring in the Atlantic sector of the Southern Ocean, *Deep Sea Res., Part II, 44*, 299-320, 1997.

Eppley, R. W., Temperature and phytoplankton growth in the sea, *Fish. Bull., 70*, 1063-1085, 1972.

Eppley, R.W., F.M.H. Reid, and J.D.H. Strickland, Estimates of phytoplankton crop size, growth rate, and primary production, *The ecology of the Plankton off La Jolla California in the Period April Through September, 1967,* edited by J.D.H. Strickland, *Bull. Scripps Inst. of Oceanogr., 17*, 33-42, 1970.

Fitzwater, S.E., G.A. Knauer, and J.H. Martin, Metal contamination and its effect on primary production measurements, *Limnol. Oceanogr., 27*, 544-551., 1982.

Frost, B.W., Effects of size and concentration of food particles on the feeding behavior of the marine planktonic copepod *Calanus pacificus,. Limnol. Oceanogr., 17*, 805-815, 1972.

Fryxell, G.A., and I. Kaczmarska, Specific variability in Fe-enriched cultures from the equatorial Pacific, *J. Plankton Res., 16*, 755-769, 1994.

Gregg, W.W., and K.L. Carder, A simple spectral solar irradiance model for cloudless maritime atmospheres, *Limnol. Oceanogr., 35*, 1657-1675, 1990.

Helbling, E.W., V. Villafañe, and O. Holm-Hansen, Effect of iron on productivity and size distribution of Antarctic phytoplankton, *Limnol. Oceanogr., 36*, 1879-1885, 1991.

Kirk, J.T.O., *Light and Photosynthesis in Aquatic Ecosystems,* 509 pp., Cambridge Univ. Press, New York, 1994.

Klaas, C., Microprotozooplankton distribution and their potential grazing impact in the Antarctic Circumpolar Current, *Deep Sea Res., Part II, 44*, 375-393, 1997.

Landry, M.R., and R.P. Hassett, Estimating the grazing impact of marine micro-zooplankton, *Mar. Biol., 67*, 283-288, 1982.

Landry, M.R., B.C. Monger, and K.E. Selph, Time-dependency of microzooplankton grazing and phytoplankton growth in the subarctic Pacific, *Prog. Oceanogr., 32*, 205-222, 1993.

Landry, M.R., J. Constantinou, and J. Kirshtein, Microzooplankton grazing in the central equatorial Pacific during February and August, 1992, *Deep-Sea Res., Part II, 42*, 657-671, 1995.

Landry, M. R., et al., Iron and grazing constraints on primary production in the central equatorial Pacific: An EqPac synthesis, *Limnol. Oceanogr., 42*, 405-418, 1997.

Landry, M.R., S.L. Brown, L. Campbell, J. Constantinou, and H. Liu, Spatial patterns in phytoplankton growth and microzooplankton grazing in the Arabian Sea during monsoon forcing, *Deep Sea Res., Part II, 45*, 2353-2368, 1998.

Landry, M.R., J. Constantinou, M. Latasa, S.L. Brown, R.R. Bidigare, and M.E. Ondrusek, The biological response to iron fertilization in the eastern equatorial Pacific (IronEx II), III. Dynamics of phytoplankton growth and microzooplankton grazing, *Mar. Ecol. Prog. Ser., 201*, 57-72, 2000.

Latasa, M., R.R. Bidigare, M.E. Ondrusek, and M.C. Kennicutt II, HPLC analysis of algal pigments: A comparison exercise among laboratories and recommendations for improved analytical performance, *Mar. Chem., 51*, 3115-3124, 1996.

Latasa, M., M.R. Landry, L. Schlüter, and R.R. Bidigare, Pigment-specific growth and grazing rates of phytoplankton in the central equatorial Pacific, *Limnol. Oceanogr., 42*, 289-298, 1997.

Letelier, R.M., M.R. Abbott, and D.M. Karl, Chlorophyll natural fluorescence response to upwelling events in the Southern Ocean, *Geophys. Res. Lett., 24*, 409-412, 1997.

Li, W.K.W., Particles in "particle-free" seawater: Growth of ultraplankton and implication for dilution experiments, *Can. J. Fish. Aquat. Sci., 47*, 1258-1268, 1990.

Löscher, B.M., H.J.W. De Baar, J.T.M. De Jong, C. Veth, and F. Dehairs, The distribution of Fe in the Antarctic Circumpolar Current, *Deep Sea Res., Part II, 44*, 143-187, 1997.

Measures, C. I., and S. Vink, Dissolved Fe in the upper waters of the Southern Ocean during the 1997/98 US-JGOFS cruises, *Deep Sea Res., Part II*, in press, 2001.

Miller, C.B., B.W. Frost, P.A. Wheeler, M.R. Landry, N. Welschmeyer, and T.M. Powell, Ecological dynamics in the subarctic Pacific, a possibly iron-limited ecosystem, *Limnol Oceanogr., 36*, 1600-1615, 1991.

Mitchell, B.G., E.A. Brody, O. Holm-Hansen, C. McClain, and J. Bishop, Light limitation of phytoplankton biomass and macronutrient utilization in the Southern Ocean., *Limnol. Oceanogr., 36*, 1662-1677, 1991.

Monger, B.C., and M.R. Landry, Flow cytometric analysis of marine bacteria with Hoechst 33342, *Appl. Environ. Microbiol., 59*, 905-911, 1993.

Moore, J. K., M.R. Abbott, J.G. Richman, W.O. Smith, T.J. Cowles, K.H. Coale, W.D. Gardner, and R.T. Barber, SeaWiFS satellite ocean color data from the Southern Ocean, *Geophy. Res. Lett., 26*, 1465-1468, 1999.

Nelson, D.M., and W.O. Smith Jr., Sverdrup revisited: Critical depths, maximum chlorophyll levels, and the control of Southern Ocean productivity by the irradiance-mixing regime, *Limnol. Oceanogr., 36*, 1650-1661, 1991.

Price, N.M., B.A. Ahner, and F.M.M. Morel, The equatorial Pacific Ocean: Grazer-controlled phytoplankton populations in an iron-limited ecosystem, *Limnol. Oceanogr., 39*, 520-534, 1994.

Putt, M., and D.K. Stoecker, An experimentally determined carbon:volume ratio for marine "oligotrichous" ciliates from estuarine and coastal waters, *Limnol. Oceanogr., 34*, 1097-1103, 1989.

Scharek, R., M.A. Van Leeuwe, and H.J.W. De Baar, Responses of Southern Ocean phytoplankton to the addition of trace metals, *Deep Sea Res., Part II, 44*, 209-227, 1997.

Sherr, E.B., and B.F. Sherr, Preservation and storage of samples for enumeration of heterotrophic protists, Handbook of Methods in Aquatic Microbial Ecology, edited by P.K. Kemp et al., pp. 207-212, CRC Press, Boca Raton, Fla., 1993.

Smetacek, V., H.J.W. De Baar, U.V. Bathmann, K. Lochte, and M.M. Rutgers van der Loeff, Ecology and biogeochemistry of the Antarctic Circumpolar Current during austral spring: A summary of Southern Ocean JGOFS cruise ANT X/6 of R.V. *Polarstern*, *Deep Sea Res., Part II, 44*, 1-21, 1997.

Strathmann, R.R., Estimating the organic carbon content of phytoplankton from cell volume or plasma volume, *Limnol. Oceanogr., 12*, 411-418, 1967.

Strom, S., and N.A. Welschmeyer, Pigment-specific rates of phytoplankton growth and microzooplankton grazing in the open subarctic Pacific Ocean, *Limnol. Oceanogr., 36*, 50-63, 1991.

Vaulot, D., C. Courties, and F. Partensky, A simple method to preserve phytoplankton for flow cytometric analyses, *Cytometry, 10*, 629-635, 1989.

Veth, C., I. Peeken, and R. Schrek, Physical anatomy of fronts and surface waters in the ACC near 6°W meridian during austral spring 1992, *Deep Sea Res., Part II, 44*, 23-49, 1997.

Wright, S.W., S.W. Jeffrey, R.F.C. Mantoura, C.A. Llewellyn, T. Bjornland, D. Repeta, and N. Welschmeyer, Improved HPLC method for the analysis of chlorophylls and carotenoids from marine phytoplankton, *Mar. Ecol. Prog. Ser., 77*, 183-196, 1991.

M.R. Abbott and R.M. Letelier, College of Oceanic and Atmospheric Sciences, Oregon State University, Corvallis, OR 97331-5503.

R.R. Bidigare, S.L. Brown, S. Christensen, M.R. Landry, and K.E. Selph, Department of Oceanography, University of Hawaii at Manoa, 1000 Pope Rd., Honolulu, HI 96822 (landry@soest.hawaii.edu)

K. Casciotti, Geosciences Department, Guyoy Hall, Princeton University, Princeton, NJ, 08544.

(Received December 23, 1999; revised November 30, 2000; accepted December 11, 2000)